Uncertainty Modeling and Robust Analysis of Atmospheric Launchers: Incremental Steps for Industrial Transfer ⋆

Andres Marcos * **Samir Bennani** ** **Christophe Roux** *** **Monica Valli** ***

* *University of Bristol, BS8 1TR, United Kingdom (andres.marcos@bristol.ac.uk).*
** *ESA-ESTEC, Noordwijk, 2201AZ, The Netherlands (e-mail: samir.bennani@esa.int)*
*** *ELV, Rome, 00034, Italy (e-mail: Christophe.Roux@elv.it, Monica.Valli@consultant.elv.it)*

Abstract: Nowadays Linear Fractional Transformations (LFT) and the Structured Singular Value (mu) are very well established concepts for respectively modeling uncertain systems and to perform robust analyses. Despite their ample use in academia and industry during the last 30 years, and the availability of consolidated software toolboxes, their introduction to a new industrial collaborator is not without angst. In this article, the steps followed to transfer this technology to the GNC group at ELV, in charge of the VEGA atmospheric launcher, are presented. The aim of the transfer was to introduce worst-case analysis tools into the VEGA verification and validation process as a complement to the standard LTI gain/phase margin analyses and the nonlinear simulation-based Monte Carlo campaigns. The successful transfer hinged on the reconciliation of the following two facets: (i) the physical behavior of the system with the LFT model capabilities, and (ii) the classical design experience from the VEGA GNC group with the results from the robust mu analyses.

Keywords: LFT modeling, robust analysis, worst-case, launcher

1. INTRODUCTION

A concept widely used in robust control is the structured singular value μ, which analytically evaluates the robustness of uncertain systems Doyle, J. (1982); Doyle, J. et al. (1991); Packard, A. and Doyle, J. (1993); Zhou, K. et al. (1996). A key aspect on the application of μ is the development of a proper LFT model. By proper it is meant a model that captures the critical parametric behavior of the nonlinear system under consideration within a complexity that still enables the application of the μ analysis algorithms.

LFTs and μ have been used in academia and industry during the last 30 years, basically since the appearance of the first version of the toolbox from Balas, G.J. et al. (1998) in July 1993. Its introduction to industry was very quick following a series of hands-on workshops by the developers at a number of companies dealing with complex, uncertain systems, e.g. aerospace. The use of these concepts, methods and tools was consolidated through practice and nowadays is ingrained in those industrial groups that have had the necessity and opportunity, for example for satellites (see references Charbonnel, C. (2010); Pittet, C. and Arzelier, D. (2006)) and the European Automated Transfer Vehicle (ATV), reference Ganet-Schoeller, M. et al. (2009).

Still, despite its wide acceptance and use, it is not without difficulty to try introducing them into the design and analysis process of other industrial groups. Much of this is due to human resources reasons such as: staff rotation, experts' availability and management risk-adverse decisions. But there are also research and development hurdles, which can be summarized in two facets: (i) clear alignment of the physical behavior of the system with the LFT model capabilities, and (ii) reconciliation of classical design experience with the results from the robust μ analyses. In addition, despite well document manuals, detailed tutorials and many publications, there is always the need of a tailored-made benchmark and code scripts that must be transferred to the industrial design group in order for them to really introduce the techniques in their verification and validation (V&V) process. For example, in reference Jang, J.W. et al. (2008), by a renown group of control experts, a simple mass-spring-damper case was used to illustrate the "limitations" of μ in evaluating its potential for the Ares I launcher programme. It was claimed that μ suffered of conservativeness and had to be used with care even for this simple case. But actually, it is easy to show that if a proper LFT model is used then μ correctly identifies a worst-case right on the stability boundary of the (damping, spring) coefficients plane.

Thus, the relevance of this article is precisely in presenting the transfer of these techniques to the GNC group of VEGA, the new European Small Launch Vehicle developed under responsibility of ESA by ELV as the prime contractor –which successfully flew its 4^{th} qualification flight on 11^{th} February 2015. The benchmark selected is a simplified planar launcher motion during atmospheric phase which allows to directly connect the system behavior and results expected by the control experts at ELV with the modeling and robust analysis capabilities of LFT and the structured singular value μ.

⋆ This work was funded by ESA-ESTEC Contract No. 4000111052/14/NL/GLC/al within the project "Analytic Stochastic Time Varying Mu Analysis for the VEGA GNC"

The article layout is based on the three first steps of the process followed to accomplished the transfer:

(1) Provide a high-level theoretical description.
(2) Define a simple, but representative study case.
(3) Follow incremental, step-by-step application.
(4) Release a compact code script of the above.
(5) Collaborate: visit and support.

2. HIGH-LEVEL THEORETICAL PRESENTATION

The importance of a theoretical presentation for industrial transfer is to conceptualize the key ideas underpinning the methods and tools as opposed to provide a detailed and mathematical exact academic exposition.

2.1 Linear Fractional Transformations (LFT)

A LFT is a representation of a system using a feedback interconnection and two matrix operators, $M = [M_{11}\ M_{12};\ M_{21}\ M_{22}]$ and Δ. The matrix M represents the nominal (known) part of the system while Δ contains the parameters ρ_i measuring the unknown. The parameters ρ_i can be real or complex, as well as static, time-varying or nonlinear. There are two possible types of LFTs, lower and upper (see also Fig. 1):

$$F_L(M,\Delta) = M_{11} + M_{12}\Delta(I - M_{22}\Delta)^{-1}M_{21} \quad (1)$$

$$F_U(M,\Delta) = M_{22} + M_{21}\Delta(I - M_{11}\Delta)^{-1}M_{12} \quad (2)$$

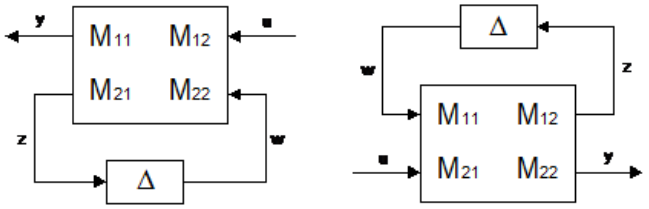

Fig. 1. Lower and upper LFTs

Of course, the LFTs are only well-defined if the inverses exist. The matrix Δ is unrestricted in form (structured or unstructured) but it is important to note that unstructured uncertainty at component level becomes structured at system level. The selection of the variable set $\rho_i \in \Delta$ that captures the behavior of the nonlinear system is a task that is not always obvious a priori. Indeed, this step is key to obtain a LFT that will yield relevant and meaningful results and, despite its apparent simplicity, is where most of the LFT modeling effort and ingenuity is focused. The goal is to achieve the correct trade-off between LFT complexity (number of ρ parameters and total dimension of Δ) versus fidelity with respect to the nonlinear system behaviour.

There are several approaches and toolboxes that facilitate obtaining a proper LFT model (see Lambrechts, P. et al. (1993); Hansson, J. (2003); Magni, J.F. (2004); Marcos, A. and Balas, G.J. (2004); Marcos, A. et al. (2007); Balas, G.J. et al. (2014) and references therein).

2.2 Structured Singular Value, μ

The structured singular value $\mu_\Delta(M)$ of a matrix $M \in C^{n\times n}$ with respect to the uncertain matrix Δ is defined in (1), where $\mu_\Delta(M) = 0$ if there is no Δ satisfying the determinant condition.

$$\mu_\Delta(M) = \frac{1}{\min_\Delta(\sigma(\Delta) : \det(I - \Delta M) = 0)} \quad (3)$$

Note that this definition is given in terms of an $\{M,\Delta\}$ model which is an LFT model where Δ is typically norm-bounded $\|\Delta\|_\infty < 1$ (without loss of generality by scaling of M) for ease of calculation and interpretation. In this manner, if $\mu_\Delta(M) \leq 1$ then the result guarantees that the analyzed system, represented by the LFT (for example an uncertain closed-loop system), is robust to the considered uncertainty level. The structured singular value is a robust stability (RS) analysis but can be used also for robust performance (RP), see [4].

Since $\mu_\Delta(M)$ is difficult to calculate exactly, the algorithms implement upper and lower bound calculations Balas, G.J. et al. (1998). The upper bound μ_{UB} provides the maximum size perturbation $\|\Delta_{UB}\|_\infty = 1/\mu_{UB}$ for which RS/RP is guaranteed, while the lower bound μ_{LB} guarantees the minimum size perturbation $\|\Delta_{LB}\|_\infty = 1/\mu_{LB}$ for which RS/RP is guaranteed to be violated. Thus, if the bounds are close in magnitude then the conservativeness in the calculation of μ is small, otherwise nothing can be said on the guaranteed robustness of the system for perturbations within $[1/\mu_{UB}, 1/\mu_{LB}]$.

Note that in the above interpretation, the one used most often, $\mu_\Delta(M)$ becomes a binomial-type of robust analysis (i.e. either the system is robust or not ($\mu_\Delta(M) \leq 1$ or > 1)), with an assessment on the conservativeness of the answer given by the range of the bounds, and returning the associated worst-case Δ at these peak values. As it will be shown later this is a simplified view on the analytical power of $\mu_\Delta(M)$ since in reality it is a worst-case frequency-domain analysis allowing to extract robust/worst-case information across frequencies.

3. STUDY CASE FOR LAUNCHER TVC

A launcher thrust vector control (TVC) example is proposed to serve as a simple, yet relevant, study case. The advantage of this case is that it contains some of the main characteristics for atmospheric launchers and facilitates understanding of the results. The (2 rigid states + 1 bending mode of 2^{nd} order) state-space system for this study case is given by:

$$A_{LV} = \begin{bmatrix} 0 & 1 & 0 & 0 \\ A_6 & 0 & 0 & 0 \\ 0 & 0 & 0 & 1 \\ 0 & 0 & -\omega_{1B}^2 & -2\zeta_{1B}\omega_{1B} \end{bmatrix};\ B_{LV} = \begin{bmatrix} 0 \\ K_1 \\ 0 \\ -Tn\,TMC_{PVP} \end{bmatrix} \quad (4)$$

$$C_{LV} = \begin{bmatrix} 1 & 0 & -RMC_{INS} & 0 \\ 0 & 1 & 0 & -RMC_{INS} \end{bmatrix};\ D_{LV} = \begin{bmatrix} 0 \\ 0 \end{bmatrix} \quad (5)$$

where TMC_{PVP} and RMC_{INS} are the bending mode's translational (at pivot point, PVP) and rotational (at the inertial navigation system, INS) lengths. The general characteristics are:

(1) *Simplified yaw planar rigid motion*. The real-uncertain rigid model is a two states / outputs [ψ, $\dot{\psi}$] containing only the aerodynamic A_6 and controllability K_1 terms and with a single input Tn thrust deflection. (A_6, K_1) are mathematical variables formed by physical parameters such as center of gravity x_{CG}, moment of inertia J_{yy}, dynamic pressure $\bar{q}$, launcher's reference area S_{ref}, yawing coefficient CN_α, center of pressure x_{CP} and pivot reference x_{PVPref}:

$$A_6 = S_{ref}\,\bar{q}\,CN_\alpha \frac{(x_{CP}-x_{CG})}{J_{yy}}; \quad K_1 = Tn\,\frac{(x_{PVPref}-x_{CG})}{J_{yy}} \tag{6}$$

(2) *Simplified bending effects*. A single 1^{st} bending mode is used based on a 2^{nd} order model with damping ζ_{1B} and frequency ω_{1B} with 20% real uncertainty, i.e. yielding an uncertain range $\Delta_{\omega_{1B}} = [20.08 - 30.12]$.
(3) *Simplified thrust vector control*. The TVC is modeled as a 2^{nd} order model that includes full complex uncertainty of about 6% ($0.5dB$) as a multiplicative weight.
(4) *Simplified time delay*. The delay is approximated by a 2^{nd} order Pade model with asymmetric real uncertainty ranging between $\Delta_\tau = [0.1 - 0.16]$ seconds.
(5) *PD attitude controller*. The controller $K(s) = K_P + K_D s$ is based on the equivalence of the $K_\#$ gains to a 2^{nd}order system with desired bandwidth ω_{des} and damping ζ_{des}.
(6) *Data at maximum $Q\alpha$ time*. The data used for the robust analyses performed in this article was extracted at maximum $Q\alpha$ from a nominal simulation of the VEGA nonlinear high-fidelity simulator using a real wind profile.

With respect to the last point, note that the standard $\mu_\Delta(M)$ robust analysis is linear-time-invariant. For launcher vehicle analysis along its time-varying atmospheric trajectory, a frozen time approach is followed whereby every x seconds along the trajectory the developed LFT model is numerically evaluated at the extracted data and the robust analysis performed to identify worst-cases at each of these points. The resulting cases are then verified and validated in the nonlinear, high-fidelity time simulators. The reader is referred to Marcos, A. et al. (2015) for further details in its application to VEGA.

Focusing on the rigid motion, the plant model can be represented by $G(s) = K_1/(s^2 - A_6)$, and assuming unity negative-feedback with the PD controller, the closed-loop transfer function is obtained (note $L(s) = G(s)K(s)$):

$$T(s) = \frac{L(s)}{I + L(s)} = \frac{K_1(K_P + K_D s)}{s^2 + K_1 K_D s + (K_1 K_P - A_6)} \tag{7}$$

Equating the above characteristic equation with an ideal 2^{nd} order system with desired bandwidth ω_{des} and damping ζ_{des}, the following general gain expressions are obtained:

$$K_P = \frac{\omega_{des}^2 + A_6}{K_1}; \qquad K_D = \frac{2\zeta_{des}\omega_{des}}{K_1} \tag{8}$$

Equation 8 shows that for a given instance of time (from which to numerically obtain A_6 and K_1 values), the control designer must only assign a desired frequency and damping to obtain the desired closed-loop behavior.

4. INCREMENTAL APPLICATION

4.1 Launcher TVC LFT models

In order to provide insight on the possibilities offered by LFT modeling, and on the impact such choices may have on the results, 4 different LFT models were derived. The difference is based on the definition of the rigid-motion uncertainty models (with those for the bending, TVC and time delay common to all LFTs). Table 1 gives per each LFT model (row), the uncertain rigid parameters/models used and total LFT dimension along the columns , with the last row providing the uncertainty models common to all.

Next, a brief description of each model significance is given:

(1) **LFT-0** represents the standard LFT modeling approach of capturing the state-space matrix coefficients variability across flight conditions and/or physical uncertainty. In the simplest case the level of variability (σ_{A_6}, σ_{K_1}) is based on prior knowledge and rules of thumb.
(2) **LFT-1** is a step up from the previous model in that now the designer is attempting to capture the variability of the physical parameters that compose the state-space matrices, albeit still defining $\sigma_\#$ based on experience.
(3) **LFT-2** is the first model where a nonlinear system assessment is used to guide the choice of uncertainty model (i.e. additive) and variability (i.e. $\sigma_\#^{dTC}$ and $\sigma_\#^{\rho}$), although still keeping the uncertain flags uncorrelated (as in LFT-2).
(4) **LFT-3** is the most realistic LFT model. The type of uncertain model, level and even uncertainty parameter (Δ_{dTc} for burning time and Δ_ρ for density) are chosen based on a methodological analysis of the influence all the uncertain parameters implemented in the nonlinear simulator of VEGA have on the physical parameters.

Note that the models represent a continuum from the simplest LFT model a designer may be tempted to use (to save modeling effort) towards a higher fidelity LFT model (which might require specific modeling effort). This represents a transference of uncertainty paralleling that in standard design cycles where initially it is assumed a large uncertainty (phase 0) which is reduced as the production phase begins. Note that even if the higher-fidelity LFT is developed, the different uncertainty models can be quite readily and easily interchanged allowing to create a library of LFT models that do not require any fundamental additional modeling effort beyond the initial one.

The available modeling choices for the present case (although are general to any LFT modeling process) can be summarized:

(1) *Type of uncertain parameters*: non-physical (e.g. matrix coefficients), physical (e.g. center of gravity, mass) or constituent (the most basic set of physical parameters from which all other parameters depend);
(2) *Type of LFT model*: multiplicative versus additive;
(3) *Level of uncertainty*: defined from experience, by approximation or from data-analysis;
(4) *Correlation of the uncertain parameters*. Note that most physical parameters tend to be correlated (e.g. center of gravity, mass and inertia) but that simpler models are obtained when these correlations are obviated.

Table 1. LFT models

LFT-#	real, rigid uncertainty $\lvert\Delta_\#\rvert \le 1$	total dim(Δ)
LFT-0	$\begin{cases} A_6 = A_6^o(1+\sigma_{A_6}\Delta_{A_6}) \\ K_1 = K_1^o(1+\sigma_{K_1}\Delta_{K_1}) \end{cases}$	10
LFT-1	$\begin{cases} J_{yy} = J_{yy}^o(1+\sigma_{J_{yy}}\Delta_{J_{yy}}) \\ x_{CG} = x_{CG}^o(1+\sigma_{x_{CG}}\Delta_{x_{CG}}) \\ \bar{q} = \bar{q}^o(1+\sigma_{\bar{q}}\Delta_{\bar{q}}) \end{cases}$	12
LFT-2	$\begin{cases} J_{yy} = J_{yy}^o + \sigma_{J_{yy}}^{dTC}\Delta_{J_{yy}} \\ x_{CG} = x_{CG}^o + \sigma_{x_{CG}}^{dTC}\Delta_{x_{CG}} \\ \bar{q} = \bar{q}^o + \sigma_{\bar{q}}^{dTC}\Delta_{\bar{q}} \end{cases}$	13
LFT-3	$\begin{cases} J_{yy} = J_{yy}^o + \sigma_{J_{yy}}^{dTC}\Delta_{dTc} \\ x_{CG} = x_{CG}^o + \sigma_{x_{CG}}^{dTC}\Delta_{dTc} \\ \bar{q} = \bar{q}^o + \sigma_{\bar{q}}^{dTC}\Delta_{dTc} + \sigma_{\bar{q}}^{\rho}\Delta_\rho \end{cases}$	14
All-LFTs	$\begin{cases} \omega_{1B} = \omega_{1B}^o(1+\sigma_{\omega_{1B}}\Delta_{\omega_{1B}}) \\ \tau = \tau^o(1+\sigma_\tau\Delta_\tau) \\ sys_{TVC} = sys_{TVC}^o(1+W_{TVC}(j\omega)\Delta_{TVC})) \end{cases}$	

In order to understand better the difference between the 4 proposed LFT models, Figure 2 shows the (A_6, K_1) regions spanned from evaluating the normalized rigid uncertainty of each LFT model at their minimum/maximum values –with the other uncertainties fixed.

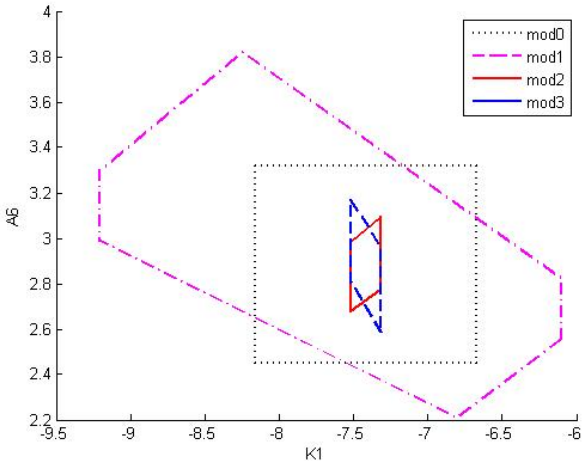

Fig. 2. K_1 vs A_6 range for all LFT models: varying only rigid Δ

It is clearly seen now the importance of more physical and correlated LFT models since a simpler uncertainty set (e.g. LFT-1) may result in an easier to get LFT model, and with smaller uncertain dimension, but at the expense of resulting in an over-bounded parameter space. The effect of having such an over-bounded space is negative from the dual perspectives of:

(1) *Design*, since the designer must ensure satisfaction of control objectives for the selected parameter space region. Thus, if it is much larger than required (i.e. larger than the actual system behavior) then the controller will need to have stronger (than necessary) robustness properties in detriment of performance.
(2) *Analysis*, since depending on the system and the type of analysis (i.e. LTI eigenvalue or gain/phase margin), more effort and time must be spent as a larger space must be analyzed –which could lead to analysis answers demanding improved robustness of the design or to partial answers not covering all the parameter space.

4.2 Robust analysis

Using the command *robuststab* from Balas, G.J. et al. (2014) it is straightforward to perform a robust stability (RS) analysis for each LFT model in Table 1 (using the indicated uncertainty parameters and levels). The analysis code used is given in Figure 3, where (*sysLV*, *sysTVC*, *sysMARGIN*, *K*) indicate respectively the systems for the launcher, the TVC actuator, the time delay and the controller:

It is well-known that μ-analysis for pure real uncertainty may present discontinuities when calculating the lower bound. This is typically avoided by performing a mixed real/complex μ-analysis but as opposed to typical usage from the command *complexify* in Balas, G.J. et al. (2014), which adds a percentage of complex value to all the parameters in the set, it is suggested to choose always the parameter with the least influence on the system. In the present case due to the full complex uncertainty used for the TVC model there is no need to complexify the uncertainty set.

```
%% Mu robust stability analysis

% Mu options
opt2     = robopt('Mussv','m3');
theOmega = logspace(-2,2,200);

% Form closed loop
sysLV_CL    = feedback(sysLV*sysTVC*sysMARGIN,-K);
sysLV_CL_fr = ufrd(sysLV_CL,theOmega);

% Perform mu RS analysis
[SM,DeUnc,rep,info] = robuststab(sysLV_CL_fr,opt2);

% Get Upper & Lower bounds
ParaUB = info.MussvBnds(1);
ParaLB = info.MussvBnds(2);

% Cross-check Worst-Case uncertainty combination
clp_DeUnc = usubs(sysLV_CL,DeUnc);
clp_DeUnc = eig(clp_DeUnc);
```

Fig. 3. Compact code for robust stability analysis

To build up confidence on the results and μ, the first RS analysis removes the bending uncertainty from the LFT models. Figure 4 shows the upper μ_{UB} and lower μ_{LB} bounds for the robust stability analysis of the four LFT models (all without the 1^{st} bending model uncertainty). It is seen that they are all robustly stable ($\mu < 1$) but more significantly all show a remarkable similar trend for both bounds. Nonetheless, the first two models (top row) provide, somehow unexpectedly, smaller bounds gap at the low frequency region while the last two (bottom row) provide closer gap around the peaks, which are also narrower. It is not possible to determine which analysis/LFT model is best, and indeed this is an open question in the field (i.e. defining and characterizing the "best" LFT model for μ analysis).

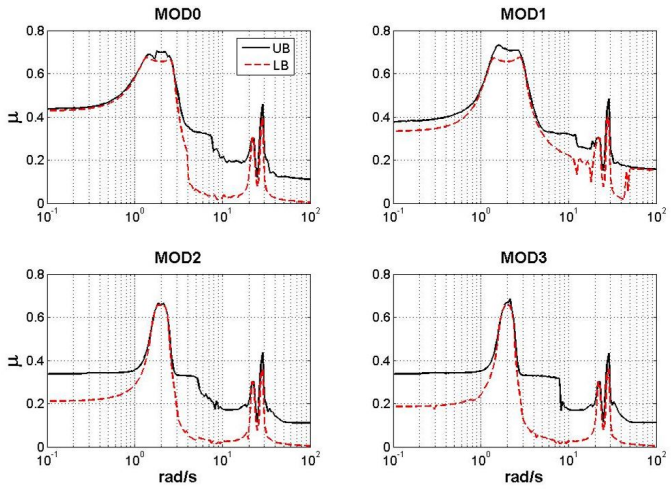

Fig. 4. μ_{RS} bounds for all LFT models with no bending Δ

Next, Figure 5 shows the values for (A_6, K_1, τ) across frequency from the uncertainty worst-cases (WC) obtained above from the μ_{LB}. Despite the previous comments on the similarity of the bounds across models, as well as the WC combinations showing similar trends, it is noted that the actual WC values are different and indeed for some cases, e.g. frequencies above 4 rad/sec for the K_1, very different. This indicates that the choice of LFT uncertain parameters and variability is key if specific worst-case identification is required but that the robust stability

results are not driven by this choice (although obviously this is very system dependent and moreover, the total LFT dimension and number of parameters can hamper the use of μ).

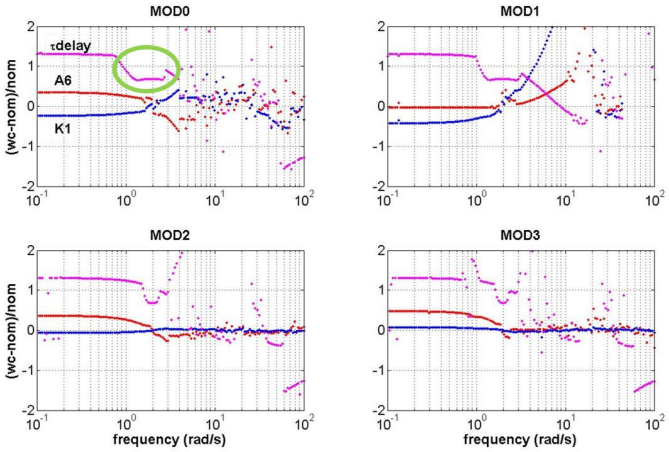

Fig. 5. WC across frequency for all LFTs with no bending Δ

Still, it is remarkable that for all the LFT models the resulting worst-case combinations seen in Figure 5 capture very well the interplay between the A_6 (red dots) and K_1 (blue dots) parameters -it is well known that for instability A_6 should tend towards positive values while K_1 towards negative. This is clearly the case for LFT-0, as expected due to its direct handle on this duplet, but still valid (albeit with different magnitudes) to all the other models. In addition, see the well correlated effect of the time delay between the dip in Figure 5 (marked by a green circle in the top-left plot) and the highest peak in Figure 4 (both around the $[10^0 - 10^{0.2}]$ frequency region).

Progressing with the analysis, the models' complexity is increased. Figure 6 shows the RS bounds for all the LFT models using now the full uncertainty set –that is, including the 1^{st} flexible mode and its uncertainty. Notice that the expected de-stabilizing effect of the bending modes is correctly picked up by μ (and around the expected frequency), and again all the LFT models show similar trend and effects.

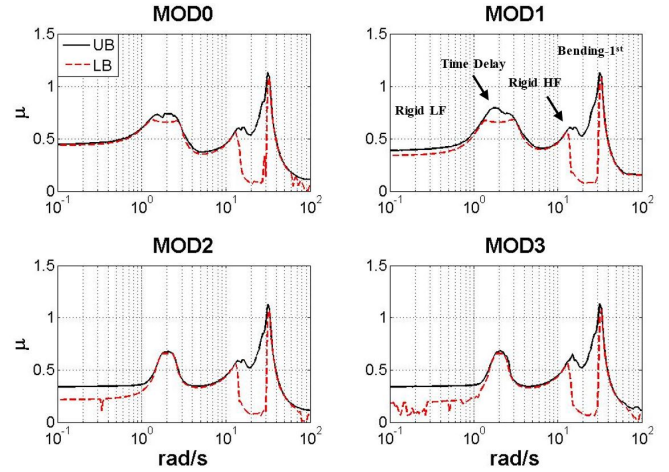

Fig. 6. μ_{RS} bounds for full Δ set

When comparing Figure 6 with its equivalent Figure 4 (without the bending mode), the de-stabilizing effect is clear. Notice that for the latter case, no robust analysis for any model yields a μ bound higher than about 0.7. This implies that for the no-bending modes case, it is possible to augment the uncertainty by about 40% (=1/0.7) its current size. On the other hand, in the flexible case it is seen that the bounds are again very close (indicating no conservativeness) and all about a μ value of 1.1 meaning that it is necessary to reduce the uncertainty by approximately 10% in order to be stable.

Further, since it is clear (from the knowledge of the system's frequency spectrum) that the uncertainty causing the instability problem is that for the bending mode, the control designer has now plenty of information to redesign the controller around that frequency region and for those effects, or to provide the analysis information to the system engineers so that the potential flexible uncertainty is limited and/or the control design objectives relaxed (if possible, i.e. not the stability objectives).

To provide a numerical assessment of the previous comments, the uncertainty values corresponding to the worst-on-worst cases (WCs, i.e. those arising from the highest lower bound peaks) for the full Δ case are given in Tables 2 and 3 for each LFT model. The (A_6, K_1) values given in the first two columns of Table 2 are obtained by substituting the WC uncertainty values from Table 3 in the corresponding equations shown in Table 1. Looking at these worst-case (A_6, K_1) values it is clear that there are slight differences arising from the different models, but too few to mention. It is also interesting to note that the uncertainty parameters common to all the LFT models, (i.e. $\Delta_{\omega_{1B}} \in [20.08 - 30.12]$ and $\Delta_\tau \in [0.1 - 0.16]$) have very similar values – Δ_{TVC} is not given as it is a full complex uncertainty.

Table 2. μ_{RS} worst-case for each LFT model

LFT-#	A_6	K_1	$\Delta_{\omega_{1B}}$	Δ_τ
LFT-0	2.53	-7.24	29.79	0.15
LFT-1	2.94	-6.53	29.78	0.15
LFT-2	3.06	-7.32	29.80	0.15
LFT-3	2.61	-7.32	29.80	0.15

Table 3. 'Cont μ_{RS} worst-case for each LFT model

LFT-#	Δ_{A_6}	Δ_{K_1}	$\Delta_{J_{yy}}$	$\Delta_{\bar{q}}$	$\Delta_{x_{CG}}$	Δ_{dTc}	Δ_ρ
LFT-0	-0.81	-0.22					
LFT-1			0.51	0.63	-0.92		
LFT-2			0.81	0.80	-0.92		
LFT-3						-0.92	-0.91

Finally, in order to provide an additional graphical measure of the lack of conservativeness of μ for this case, the identified WCs are plotted on an (A_6, K_1) stability map, see Figure 7. This map, where grey indicates stability and magenta the instability regions, is obtained using a grid of (A_6, K_1) values and assessing the eigenvalue sign of the closed-loops formed by the PD controller and each of the LFT models. The position of the nominal (A_6, K_1) value (nom) and the above worst-case (μ_{WC}) values are identified in the maps. Note that these WCs (identified as black dots and highlighted by an arrow) are always at the limit of the stable/unstable regions showcasing that μ yields a very close to the stability boundary worst-combination.

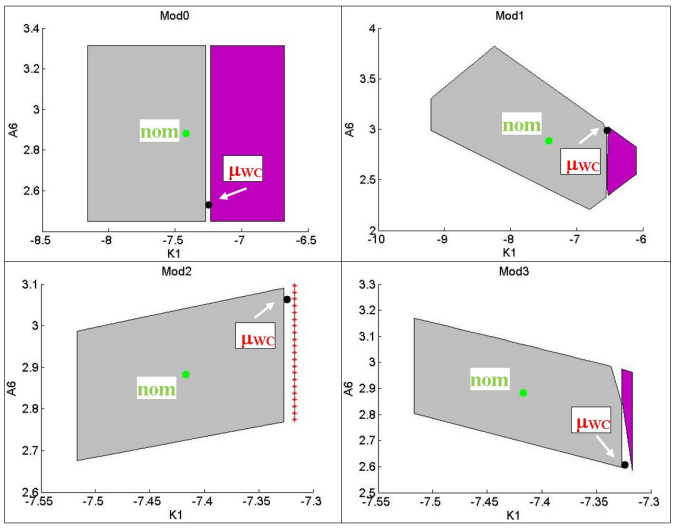

Fig. 7. (K_1, A_6) stability regions with nominal and μ_{WC} values

5. CONCLUSION

In this article, a summary of the main steps taken to transfer LFT and μ robust analysis techniques to the GNC group of VEGA is presented.

In order to succeed in such a transfer, two main issues must be addressed: (i) clear alignment of the physical behavior of the system with the LFT model capabilities, and (ii) reconciliation of classical design experience with the results from the robust μ analyses. In order to accomplish this transfer a simple study case representative of the system must be employed. Thus, for the present case, the benchmark selected is a simplified planar launcher motion during atmospheric phase. It is noted that the transfer has been successful, which included several visits to ELV for direct collaboration, and the techniques are now being employed internally –albeit not yet as part of the VEGA V&V design cycle.

It is noted that for this study case all the LFT models allowed obtaining relatively tight results for the bounds, especially for the peaks in the low frequency (associated to the launcher LF margin) and in the higher frequency (associated to the 1^{st} bending mode). This of course arises from the ample LFT expertise of the authors, but mostly from the relatively simplicity of the models (i.e. 5/6 uncertain parameters with total dimensions between 10/14). In response to potential criticism to such simplicity, it is highlighted that the LFT models are general to all launchers in atmospheric phase and share most of their intrinsic difficulties pertaining planar motion. In addition, even these simple LFT models provide a better framework for analysis than the random sampling of frozen-time points along the trajectory typically used for gain/phase margin. Thus, these models can now be used as an off-the-self library of models where testing of new controller tunings or more refined uncertainties can be carried out in a robust framework and in a matter of minutes using the compact code scripts developed.

Finally, we would like to remark that although typically only the worst-on-worst (i.e. the highest peak) uncertainty combination is used, de-stabilizing perturbations of size $|\Delta|_\infty < 1$ can be obtained for each frequency tested that yielded $\mu_{LB} > 1$. Thus, a direct region-based identification of worst-cases can be performed by using μ in this fashion. This is noted to highlight that the use of μ should not be circumscribed to a binomial examination of the robust stability/performance (i.e. whether the μ peak is above or below 1), but rather can be used very efficiently to determine evolution of worst-cases along frequency, sizing of uncertainties for system objectives update, identification of frequency regions of interest for different effects, and so on.

ACKNOWLEDGEMENTS

The authors would like to acknowledge the support of Xavier Lefort, ESA VEGA Integrated Project Team.

REFERENCES

Balas, G.J., Chiang, R., Packard, A., and Safonov, M. (2014). Robust Control Toolbox.

Balas, G.J., Doyle, J.C., Glover, K., Packard, A., and Smith, R. (1998). μ-Analysis and Synthesis Toolbox.

Charbonnel, C. (2010). H-infinity Controller Design and mu-analysis: Powerful Tools for Flexible Satellite Attitude Control. In *AIAA GNC Conference*. Toronto, Canada.

Doyle, J. (1982). Analysis of feedback systems with structured uncertainties. In *IEE Proceedings. Part D*, volume 129(6), 242–250.

Doyle, J., Packard, A., and Zhou, K. (1991). Review of LFTs, LMIs, and μ. In *IEEE Conference on Decision and Control*.

Ganet-Schoeller, M., Bourdon, J., and Gelly, G. (2009). Nonlinear and Robust Stability Analysis for ATV Rendezvous Control. In *AIAA GNC Conference*. Chicago, USA.

Hansson, J. (2003). *Using Linear Fractional Transformations for Clearance of Flight Control Laws*. Master's thesis, Department of Electrical Engineering, Automatic Control, University of Linkoping.

Jang, J.W., Van Tassell, C., Bedrossian, N., Hall, C., and Spanos, P. (2008). Evaluation of Ares I Control System Robustness to Uncertain Aerodynamics and Flex Dynamics. In *AIAA GNC Conference*. Honolulu, HA.

Lambrechts, P., Terlouw, J., Bennani, S., and Steinbuch, M. (1993). Parametric Uncertainty Modeling using LFTs. In *American Control Conference*, 267–272. San Franciso, CA.

Magni, J.F. (2004). Linear Fractional Representation Toolbox Modelling, Order Reduction, Gain Scheduling. Technical Report TR 6/08162 DCSD, ONERA, Systems Control and Flight Dynamics Department, Toulouse, France.

Marcos, A. and Balas, G.J. (2004). Development of Linear Parameter Varying Models for Aircraft. *Journal of Guidance, Control, and Dynamics*, 27(2), 218–228.

Marcos, A., Bates, D.G., and Postlethwaite, I. (2007). A Symbolic Matrix Decomposition Algorithm for Reduced Order Linear Fractional Transformation Modelling. *Automatica*, 43(7), 1125–1306.

Marcos, A., Rosa, P., Roux, C., Bartolini, M., and Bennani, S. (2015). An overview of the RFCS project V&V framework: optimization-based and linear tools for worst-case search. *CEAS Space Journal*. DOI: 10.1007/s12567-015-0092-2.

Packard, A. and Doyle, J. (1993). The complex structured singular value. *Automatica*, 29(1), 71–109.

Pittet, C. and Arzelier, D. (2006). DEMETER: a benchmark for robust analysis and control of the attitude of flexible micro satellites. In *5th IFAC symposium on Robust Control Design - ROCOND 2006*. Toulouse, France.

Zhou, K., Doyle, J.C., and Glover, K. (1996). *Robust and Optimal Control*. Prenticel-Hall, Englewood Cliffs, NJ.